Proceedings of International Conference on Heat Exchanger Fouling and Cleaning VIII - 2009 (Peer-reviewed)
June 14-19, 2009, Schladming, Austria
Editors: H. Müller-Steinhagen, M.R. Malayeri and A.P. Watkinson

Published online
www.heatexchanger-fouling.com

# THE IMPORTANCE OF SCHEDULING AND DESALTER CONTROL OF PREHEAT TRAINS OF CRUDE DISTILLATION UNITS: A CASE STUDY

**E.M. Ishiyama[1], D.I. Wilson[*1], W.R. Paterson[1], A. V. Heins[2] and L. Spinelli[3]**
[1]Department of Chemical Engineering & Biotechnology, University of Cambridge, New Museums Site, Pembroke Street, Cambridge CB2 3RA, UK, Tel: (44) 01223 334777, Fax: (0044) 01223 334796
[2] Engineering Department - YPF, Macacha Güemes 515 Piso 14, Buenos Aires, Argentina
[3]Argentinean Technology Center (CTA) –YPF, Baradero S/N (1925), Ensenada, Pcia. de Buenos Aires, Argentina
[*]Corresponding author: diw11@cam.ac.uk

## ABSTRACT

Refinery preheat trains (PHTs) are networks of heat exchangers that recover heat from product and pumparound streams and transfer it to the feed stream of the atmospheric distillation column. PHTs are key determinants of the profitability of the operation of crude distillation units (ESDU, 2000), yet PHTs suffer from chronic fouling problems. Given that complete mitigation of fouling is rarely achievable in practice, PHT operation tends to deviate from design targets. This deviation is often undesirable for associated equipment such as desalters, pump-arounds, furnaces and, in some cases, preflash towers, all of which have well defined operating envelopes.

In this work a method to control desalter inlet temperature through combined cleaning and heat exchanger bypassing is presented based on a PHT simulator described previously (Ishiyama *et al.*, 2009). The methodology is illustrated using a case study based on an industrial network subject to fouling, where the fouling rates of heat exchangers were extracted through a data reconciliation exercise. The case study scenarios highlight how a simulation-based tool can be effective in controlling desalter inlet temperature within a fouling management strategy.

## INTRODUCTION

Refineries resemble mini-economies in that they have to achieve effective use of resources, minimize energy consumption and reduce emissions in order to stay competitive in the current marketplace. In the UK alone, there are nine major refineries, processing over 1.8 million barrels of crude oil per day, consuming gigawatts of energy. Amongst the processes on a refinery, distillation has been identified as the main energy consumer, as the crude oil feed must be heated and partly vapourised as it passes from ambient temperature to around 380ºC. A large fraction of the heat required for distillation (*c*. 60-70%) is recovered from the product and pump-around streams of the distillation unit through heat exchangers (HEXs). These HEXs are usually connected together in a network called the preheat train (PHT). Many crudes give rise to fouling, which not only reduces the capacity for heat transfer, but also changes the surface roughness and cross sectional area available for flow, leading to problems with pressure drop. Consequences of fouling include (*i*) higher heating costs (with associated increases in greenhouse gas emissions); (*ii*) reduction in throughput; (*iii*) increase in capital expenditure for over-designed units; (*iv*) additional cleaning and maintenance; and, in the worst case, (*v*) plant shut-down.

HEX fouling is a common economic problem, accounting for 0.25% of the gross national product (GNP) in the highly industrialized countries (ESDU, 2000). Fouling mitigation methodologies have therefore gained wide attention, such as the use of anti-foulant chemicals, tube inserts, network revamping and manipulation of operating parameters. The complexity of the fouling problem and the variability of feedstocks has rendered it almost impossible to completely eliminate fouling in PHTs. Cleaning of fouled HEXs is still, therefore, considered to be a desirable responsive action. This raises the question of when and which units should be cleaned. This example of a *scheduling problem* has spawned a variety of numerical approaches and has attracted the attention of the numerical optimization community. (*e.g.* Georgiadis *et al*., 2000; Lavaja and Bagajewicz, 2004). The problem is combinatorial and includes non-linear models. This has prompted the development of several MINLP/MILP (Mixed Integer Non-Linear Programming/ Mixed Integer Linear Programming) methodologies which consider all possible actions over a given time period in a 'total horizon' approach. Rodriguez and Smith (2007) reported alternative simulated annealing methods.

A simpler approach, based on the 'greedy algorithm', was proposed by Samïli *et al.* (2001) as this yields satisfactory scheduling solutions and permits the use of simulations incorporating operational behaviour that would cause stability problems in a 'total horizon' approach. Heuristic methods evaluate only some of the (many) possible combinations, guided by an ad hoc search, and, whilst useful, cannot guarantee to find a global optimum (if one exists). Ishiyama *et al.* (2009) have recently reported a modified 'greedy algorithm' based on a 'merit list' approach to reduce computational time. They included model-based representations of the dynamics of fouling, in addition to the thermal and hydraulic performance of the network.

A typical refinery, however, includes units such as a desalter, flash tower and furnace which are required to operate within a constrained set of operating parameters. The operating band of these units can be critical, and the importance of good control was discussed by Polley *et al.* (2009). In this paper we explore how scheduling and temperature control can be combined in a PHT simulation for fouling management, with the particular case of a desalter.

## DESALTER

Fouling occurs throughout the PHT and different mechanisms are known to cause deposition in each section. Deposition of salts, wax and corrosion have been reported for HEXs upstream of the desalter, while chemical reaction fouling and corrosion fouling are dominant downstream of the desalter (Crittenden *et al.*, 1992). Desalting, as the name implies, is intended to remove inorganic materials from the oil. Desalter malfunction hinders crude oil processing in several ways: (*i*) formation of inorganic/organic acids downstream of the desalter, causing corrosion, (*ii*) deposition of salts as mineral scale in HEXs, (*iii*) deactivation of catalysts and (*iv*) two-phase flow downstream of the desalter arising from water vapourisation.

Desalting consists of two processes; (*a*) formation of an emulsion by mixing oil with water and transfer of the ionic material to the aqueous phase, and (*b*) separation of water droplets from the oil, accelerated by electrostatic precipitation. Separation is governed by the droplet settling velocity, given by Pruneda *et al.* (2005) as

$$u_s = \frac{2gr^2(\rho_w - \rho_{oil})}{9\mu_{oil}} \quad (1)$$

Here $u_s$ is the settling velocity, $g$ is the gravitational acceleration, $r$ is the droplet radius, $\mu_{oil}$ is the viscosity of oil, $\rho_{oil}$ is the density of crude oil, and $\rho_w$ is the density of water.

Equation (1) shows that desalter operation is dependent on the operating temperature via the viscosity and density. A higher temperature promotes settling via the reduced viscosity but it also increases the electrical conductivity of the mixture. A high conductivity will result in increased voltage gradients between the electrodes, increasing the electricity cost, and in the worst case cause short-circuiting and desalter breakdown. A low temperature decreases the settling velocity and can reduce the unit throughput. Both the above effects are undesirable, so upper and lower temperature bounds are often specified for a desalter operations. Pruneda *et al.* (2005) reported a detailed model of desalter operation and used this to optimize the performance of the unit.

## NETWORK SIMULATION

Preheat trains are complex. Fouling rates are often non-linear in temperature and velocity dependency, so it is often impossible to derive analytical solutions describing network performance. The network simulator based on MATLAB and Excel described by Ishiyama *et al.* (2009) was modified here for evaluation of scheduling and control actions.

### Heat transfer

The majority of the HEXs used in PHTs are shell-and-tube devices. The performance of individual HEXs were evaluated using lumped parameter models, as in most network simulation studies, in effect assuming uniform thermal properties, heat transfer coefficients, and single phase flow. The *NTU*-effectiveness ($\varepsilon$) method is used to calculate the duty and outlet temperatures for each HEX using standard equations (*e.g.* Hewitt *et al.*, 1994). This method lends itself to simulating the thermal performance of the PHT network, as the inlet and outlet temperatures from each HEX appear in simultaneous linear equations which can be written in matrix form and solved rapidly (see Smaïli *et al.*, 2001).

### Fouling

Fouling is assumed to occur only on the tube-side, partly because reliable models for shell-side fouling of non-crude streams are not currently available. However, shell-side fouling effects could be readily incorporated in the simulation. Determining the contribution from shell-side fouling when only heat transfer data are available for reconciliation is infeasible as the problem is underspecified. The fouling rate, $\dot{R}_f$ , is calculated here using one of the 'fouling threshold' models presented by Polley *et al.* (2002).

$$\dot{R}_f = max\left\{0,\ aRe^{-0.66}Pr^{-0.33}\exp\left(-E/RT_{film}\right) - b\tau_w\right\} \quad (2)$$

where $a$ and $b$ are dimensional constants which establish the timescale of the process; $\tau_w$ is the wall shear stress on the inner tube/foulant surface, $T_{film}$ the tube-side film temperature, and $E$ and $R$ are the activation energy and the gas constant, respectively. For some of the exchangers in the case study, however, the simpler constant (linear) fouling rate model proves suitable.

The Reynolds number, $Re$, is calculated via

$$Re = \frac{u_m(d_i - 2\delta)}{\upsilon} \quad (3)$$

$u_m$ being the corrected axial mean velocity in the heat exchanger tube with the new reduced cross-sectional area; $d_i$ is the tube internal diameter; $\delta$ is the deposit thickness; $\upsilon$ is the kinematic viscosity. Evaluation of $\delta$ is detailed based on a thin-slab approximation is detailed in Ishiyama *et al.*, 2009. All the thermo-physical properties of the crude oil associated with a particular HEX are calculated at the arithmetic mean temperature of the crude oil at the HEX inlet and outlet. Likewise the Prandtl number, $Pr$, for the crude is defined via $Pr = C_p\mu_{oil}/\lambda_{oil}$, with $C_p$ being the crude specific heat capacity, $\mu_{\text{oil}}$ its dynamic viscosity and $\lambda_{\text{oil}}$ the thermal conductivity.

In Eq. (2), $\tau_w$ is not likely to vary markedly across a HEX but $T_{\text{film}}$ is, and so the average fouling rate in the unit is evaluated using the exponential integral approach presented by Ishiyama *et al*. (2008).

At any instant, the overall heat transfer coefficient, $U$, in a HEX is calculated using

$$\frac{1}{UA_{i,cl}} = \frac{1}{A_{i,f}h_i} + \frac{1}{A_o h_o} + \frac{R_f}{A_{i,cl}} + \frac{R_w}{A_o} \tag{4}$$

where $A_{i,cl}$ is the internal (clean) surface area, $A_{i,f}$ is the internal surface area after fouling, $A_o$ is the external surface area of the tube, $R_f$ the (tube-side) fouling resistance and $R_w$ the tube-wall resistance; $h_i$ and $h_o$ are the internal and the external film heat transfer coefficients, respectively. When there is variation in tube-side flow velocity, the effect of flow rate on the film heat transfer coefficient is included using standard correlations. For $h_i$, the correlation developed by Gnielinski (1976) is used with the tube-side Fanning friction factor evaluated for surface roughness, and flow velocity, using the explicit form of the Colebrook-White reported by Sousa *et al.*, (1999). It is assumed that there is no fouling on the shell-side. Initial values for the external heat transfer coefficient were calculated using standard methods (Bell-Deraware method).

The dynamics of the network are evaluated by piece-wise integration in time. At any instant, $t$, the fouling resistance in each HEX is evaluated, the coefficients in the NTU-$\varepsilon$ expressions updated and the network temperature field updated. Application of the simple Euler method

$$R_{f,t} = R_{f,t-\Delta t} + \left.\frac{dR_f}{dt}\right|_{t-\Delta t} \cdot \Delta t \tag{5}$$

can generate problems if the time period, $\Delta t$, is too coarse: the fouling rate will often slow down dramatically as deposit accumulates (for instance, as a result of changes in $T_{\text{film}}$) but this would not be captured and the effect of fouling would be over-estimated. Very short time-steps are computationally undesirable, but identifying the optimal value of $\Delta t$ is complicated by the fact that HEXs foul at different rates, and the rank order of rates may change over the time span of the problem. Hence an adaptive step-size algorithm for determining $\Delta t$ implemented by Ishiyama *et al*. (2009) was used in this work.

**Scheduling of cleaning actions**

HEXs may be isolated from service for cleaning, incurring an initial penalty in terms of heat transfer and network operability, in return for a longer term gain in heat duty and reduction in pressure drop. Scheduling cleaning in a PHT commonly employs cost-based objective functions extending over the operating time span (Rodriguez and Smith, 2007).

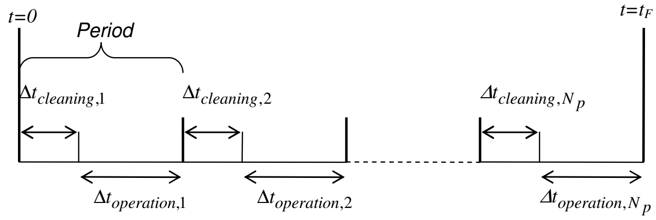


Fig. 1 Time discretisation (formulation of scheduling).

Solution of the scheduling problem employed here is based on discretisation of the operating time span into $N_p$ regular periods of months, which are divided into sub-periods for cleaning, of length $\Delta t_{\text{cleaning}}$ (7days) and operation, $\Delta t_{\text{operation}}$, as indicated in Figure 1. The optimisation approach uses a simple – and robust – 'greedy' algorithm, (GrA), which considers the cleaning actions allowed in the current period (say, $t_j$) and the impact of this action over a 'sliding' horizon, $\Delta t_w$, consisting of $N_s$ periods into the future.

Evaluating the objective function requires simulating the network over several time periods and we employ a shortcut 'merit list' algorithm to identify favourable candidates to be compared in a full simulation. For brevity in this paper only the simulations based on constant throughput are considered. At the start of each time period, the performance of the network at its current, fouled, condition is evaluated. The improvement obtained from cleaning each HEX at that point is estimated and the difference between the two is used to generate an estimated benefit:

$$\gamma_i\big|_j = \left\{C_E \cdot \left(\varepsilon_{i,cl} - \varepsilon_{i,f}\right) Q_{HEX\ i,cl} + C_{de} \cdot P_{de}\right\} \cdot \Delta t_w \tag{6}$$

Here, $\gamma_{ij}$ is the estimated benefit from cleaning HEX $i$ at period $j$, carrying the benefit forward over a time window of length $\Delta t_w$ and ignoring losses incurred during cleaning, $\varepsilon_{i,cl}$ the effectiveness of HEX $i$ when clean, $\varepsilon_{i,f}$ its current, (possibly) fouled effectiveness, and $Q_{HEX,i,cl}$ the heat duty of HEX $i$ in the clean state, $C_E$ the energy cost, and $C_{de}$ a desalter penalty cost in units of US$/(desalter penalty$\times$ day). $P_{de}$ is the desalter penalty, written as

$$P_{de} = \left[\frac{\left(T^* - T\right)}{\left(T^H - T^L\right)}\right]^n \tag{7}$$

where $T^*$ is the target temperature, $T$ the current temperature, $T^H$ the upper limit of the desalter operating range, $T^L$ is the lower limit, and $n$ is a skewness index. $n$ = 2 here, but any positive even integer could be used. Pruneda *et al.* (2005) described a more complex penalty function requiring detailed knowledge of the crude oil properties. The advantages and constraints of using penalty and barrier functions has been discussed elsewhere (Fiacco and McCornick ,1968). Our $P_{\text{de}}$ function is simpler and of a general form: the cost is framed as a deviation scaled by a penalty, the size of which is set by management considerations.

Detailed simulations are performed for the three highest ranked HEXs in the merit list, over the sliding time window. The GrA decision parameter, $G_i|_j$, is calculated for each of the selected units from

$$G_i\Big|_j = \int_{t_j}^{t_{j+N_s}} C_E\left\{Q_{ne}(t)\Big|_{no\,\text{cleaning}} - Q_{ne}(t)\Big|_{\text{clean i in period j}}\right\}dt + \int_{t_j}^{t_{j+N_s}} C_{de}\{P_{de}\}dt - C_{c,i} \tag{8}$$

$C_{c,i}$ is the cleaning cost for HEX $i$, $N_s$ is the time horizon, $Q_{ne}(t)$ is the heat duty of the network at time $t$ where the network heat duty is calculated as the sum of the heat duties of the individual heat exchangers. Subscripts '*no clean*' and '*clean i in period j*' refers to no cleaning action and the cleaning of HEX $i$ at period $j$, respectively. The sliding time horizon is truncated when it exceeds $t_F$ , *i.e.* when $t_{j+Ns}$ > $t_F$, then $t_{j+Ns}$ = $t_F$. There are other methodologies for handling the approach to $t_F$ in this scheduling problem, which were discussed by Ishiyama *et al.* (2009). A benefit threshold is set, *viz.*

$$G_i\Big|_j > \Delta G \tag{9}$$

where $\Delta G$ is the 'greedy threshold' value and in practice will be some multiple of the cost of cleaning the exchanger. The HEX with the highest $G$ value satisfying Eq. (9) is selected for cleaning in period $j$, and the algorithm then moves on to period $j$+1.

One could select more than one exchanger for cleaning in a sub-period, either simultaneously or in sequence. This requires a straightforward adaptation of the algorithm used here, although it would considerably complicate more sophisticated mathematical optimization approaches (see Wilson *et al.*, 2000).

The total network fouling penalty function, $\Gamma$, is calculated after the final period using Eq. (10) for comparison of different scenarios, such as the benefit of performing cleaning compared to taking no cleaning action.

$$\Gamma = \int_0^{t_F} \left\{ \begin{array}{l} C_E \cdot \left(Q_{ne}(t)\Big|_{no\,\text{cleaning}} - Q_{ne}(t)\Big|_{\text{clean i in period j}}\right) \\ + C_{de}\cdot P_{de} \end{array} \right\} dt + \sum_{i=1}^{all\ \text{HEX}} C_{c,i}\cdot N_{c,i} \tag{10}$$

Here, $N_{c,i}$ is the number of cleaning actions performed for HEX '$i$'.

**Desalter inlet temperature control**

One of the most common strategies for controlling the exit temperature from a HEX is to bypass part of the cold or hot stream. In most shell-and-tube units where the crude is on the tube-side, the shell-side stream is bypassed as bypassing part on the crude side would reduce the tube-side velocity, promoting a higher fouling rate (see Eq. (2)). In the following discussion the unit used for manipulation of the desalter inlet temperature, $T_{de}$, is termed the 'control HEX'.

When the control HEX is clean $T_{de}$ is likely to be high and the hot stream will be split to achieve the target $T_{de}$ value. This bypass fraction, $x$, will decrease as the control HEX (and network) is subject to fouling. It is possible to control $T_{de}$ up to a point where the bypass is fully closed (*i.e.* $x$ = 0). To simplify the calculation (primarily to reduce computational time), it is approximated that the relationship between the parameters is linear, *viz.*

$$T_{de} = c + d\cdot x \tag{11}$$

At each time step, parameters $c$ and $d$ are obtained by simulation. The bold and dashed lines in figure 2 shows loci of Eq. (11) in clean and fouled states, respectively. Solving for parameters $c$ and $d$ to obtain Eq. (11) at each fouled state involves solving a simultaneous equation with two sets of values for $T_{de}$ and $x$. Values of $T_{de}$ and $x$ at the current period and values when $x$ is zero (simulated) are used for this purpose. After obtaining the linearized form, the split fraction required to obtain the desired desalter inlet temperature is obtained through extrapolation (see Figure 2).

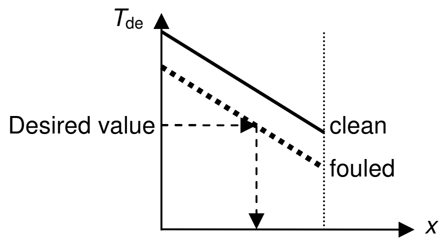


Fig. 2 Schematic of the linearized relationship between desalter inlet temperature and bypass fraction of control HEX.

**CASE STUDY**

Figure 3 shows a PHT network consisting of 18 HEXs, resembling an existing refinery in Argentina. The PHT includes a desalter and a flash tower. The HEX design parameters are listed in Table 1 and the thermo-physical properties of the crude summarized in Table 2. Heat exchangers sharing a common numeric value have the same fluid on the hot-side. e.g. the heavy gas oil (HVGO) goes through the four HEXs numbered 8, from 'A' to 'D'. The HEXs just located upstream of the desalter (*i.e.* 6A,B) are taken to be the control HEXs for the desalter, as discussed in the following section.

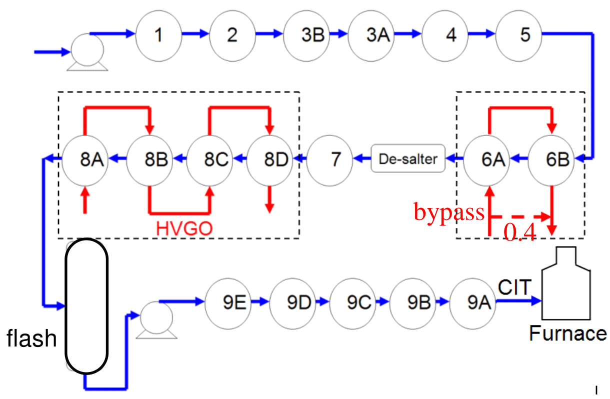


Fig. 3 Case study network consisting of 18 HEXs. CIT is the coil inlet temperature. HEXs 6A, B are used to control the desalter inlet temperature.

This study involved three stages: (*i*) data reconciliation, *(ii)* extraction of fouling rates, and (*iii*) simulating different management scenarios. The approach is a general one and could be applied to any operating PHT.

**(i) Data reconciliation**

In this step, plant operational data are inspected to obtain reliable estimates of operating parameters and performance measures (such as fouling resistance, $R_f$, -time profiles). Data filtering involved two steps:

(*a*) Removal of data over periods of 'process upset', such as when a unit was taken off-line for cleaning.

(*b*) Selection of reliable data, in this case based on a heat balance. Only data points where the heat duties of the hot and cold streams matched within a specified error limit were selected.

The error limit for the heat duty in each individual HEX was calculated from the individual uncertainties involved in flow and temperature measurements and thermo-physical properties:

$$\left(\frac{dQ_c}{Q_c}\right)=\sqrt{\left(\frac{dm_c}{m_c}\right)^2+\left(\frac{dC_{p,c}}{C_{p,c}}\right)^2+\left(\frac{d\left(T_{c,out}-T_{c,in}\right)}{\left(T_{c,out}-T_{c,in}\right)}\right)^2} \quad (12)$$

$$\left(\frac{dQ_h}{Q_h}\right)=\sqrt{\left(\frac{dm_h}{m_h}\right)^2+\left(\frac{dC_{p,h}}{C_{p,h}}\right)^2+\left(\frac{d\left(T_{h,in}-T_{h,out}\right)}{\left(T_{h,in}-T_{h,out}\right)}\right)^2} \quad (13)$$

Here subscripts *c* and *h* refer to the cold and hot streams, respectively, and the relative error terms $dY_i/Y_i$ refer to (in order) heat duty, mass flow rate, heat capacity and temperature change.

An example of the heat duty comparison for HEX 9D is plotted in Figure 4. Data points lying within the specified region between the two dashed lines were considered reliable, and taken forward for performance evaluation. Some heat exchanger data sets yielded more reliable data than others. The percentage of data acceptance ranged from 30-85%.

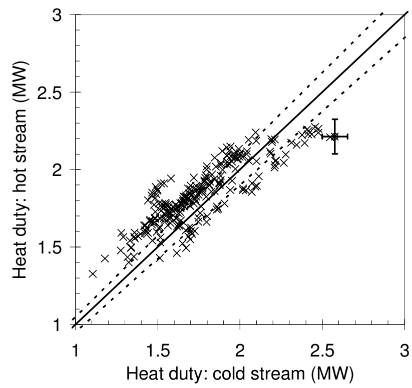


Fig. 4 Calculated duties of hot and cold streams in HEX 9D. Solid line represents of equality and dashed line represents error range generated by Eqs. (12) and (13). Error bar marked on datum indicates uncertainty in data values.

**(ii) Extraction of fouling rates**

Refinery operating data collected over a 9 month period were filtered and used to generate $R_f$-$t$ plots for each exchanger. Regression tools were used to fit each profile to one of the three fouling resistance and fouling rate trends summarized in Table 3.

The fouling resistance models in Table 3 represent commonly reported trends and are **not** employed here as fouling models *per se*: rather, they are constructions used to interpolate the data for use in fouling model comparisons. All are continuous and differentiable to yield estimates of the local fouling rate. Regression analysis yielded the dimensional constants for the most satisfactory trend line and the fouling rate could then be estimated for instants when reliable flow and temperature measurements were available.

Chemical reaction fouling is expected to be the dominant mechanism in heat exchangers located downstream of the desalter. The fouling rates obtained for these units are compared against the maximum film temperature in the unit and the average tube flow velocity in Figure 5. HEXs 7 and 9A-E show an increase in fouling rate with increasing film temperature and decreasing flow velocity, as described by the Ebert-Panchal fouling model [Eq. (2)]. This equation was fitted to the data sets and the result is plotted as a plane in Figure 5: good agreement is evident. The parameters obtained are presented in Table 4.

The extracted activation energy, 36.4 kJ mol$^{-1}$, is very similar to that reported by Crittenden *et al.* (1992) for 'light' crude oils (~33 kJ mol$^{-1}$). [Yeap *et al.* (2004) analysed a range of fouling data sets from refineries and pilot plant studies and reported activation energies ranging from 28-86 kJ mol$^{-1}$]. The above value (36 kJ mol$^{-1}$) presents a region of mixed chemical and physical fouling mechanisms, where the physical mechanism could be due to diffusion. The calculation of activation energy involves an estimation of the film and surface temperatures, which are calculated from the overall and film heat transfer coefficient values. The uncertainties involved in determining $U$ will affect the accuracy of the film and surface temperatures, and any parameters relying on these. This could also serve to reduce the activation energy.

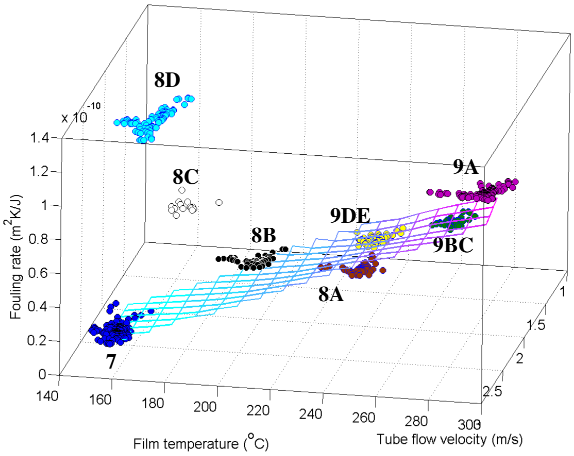


Fig. 5 Comparison of fouling rates in exchangers located downstream of the desalter. The surface indicates the best fit given by the Ebert-Panchal model [Eq. (2)] for the data in HEXs 7, 9A-E. The reported parameters indicate lumped parameter values.

Anomalous behaviour is evident in HEX 8B-D. This fouling behaviour could be due to, (a) anomalities in desalter operation or (b) shell-side fouling. The shell-side fluid here is HVGO. Li and Watkinson (2008) reported HVGO causing fouling while being heated, but this is not the case here as the HVGO is being cooled. Further work is required to elucidate this behavior.

## SIMULATIONS AND DISCUSSION

The fouling rates obtained in the previous section were used in predictions of network performance. The network initially has a coil inlet temperature, CIT, of 275°C, clean network heat duty of 67 MW, desalter inlet temperature of 130°C and a desalter operating band of 128 – 132°C. Three scenarios are compared under this case study, namely:

I. Base case - without cleaning or bypass control.
II. Cleaning only (no bypass control).
III. Combined (cleaning and bypass control).

The scheduling simulations cover an operating period of 3 years, starting from the clean state; a HEX cleaning cost of 10,000 US$/unit; a greedy threshold value of 10,000 US$; energy cost, $C_E$, of 500 US$/MWday and a desalter penalty cost, $C_{de}$, of 500US$/day.

If the network is operated without any stream temperature control or cleaning (Case I), Figure 6 shows that the coil inlet temperature, CIT, drops by 18 K over 3 years, and $T_{\rm de}$ will lie outside the desired operating band after 12 months of operation. Analysis of the fouling penalty cost in Table 5 (for Case I) gives that the additional energy cost associated with fouling represent 85% of the total fouling cost; the rest accounts for the desalter penalty.

Control of the desalter inlet temperature could be performed by scheduling cleaning actions alone (Case II) or by the combination of scheduling and bypass control (shell-side) of the control HEX (Case III). We consider Case II first. When the shell-side bypass fraction is fixed, Figure 6(b) and 6(d) show that the scheduling algorithm has focused on cleaning the units immediately before the desalters, cleaning them 3 times. It is unable to maintain $T_{\rm de}$ on target after 13 months. Figure 6 shows no cleaning actions nearing the end of the operating period. This is due to the formulation of the objective function, wherein the time period for calculating benefit of cleaning is truncated to the end of the operating period.

In Case II the shell-side stream of the two HEXs before the desalter (HEXs 6A and 6B, see Figure 3) is bypassed with a constant fraction of 0.4. In Case III, however, the shell-side bypass fraction can be changed to control the desalter inlet temperature. The shell-side bypass fraction can be manipulated under different control objectives; such as maintaining $T_{\rm de}$ at (i) the lower threshold, (ii) some mean temperature (*e.g.* the average of the lower and upper thresholds) and (iii) the upper threshold. Simulation results from each scenario indicated similar performance for all three scenarios over the 3 years of network operation, with an average CIT of 265°C, average desalter inlet temperature of 128°C and $T_{\rm de}$ able to be maintained within the control band for up to 26 months. In terms of practicality and implementation, control objective (ii) is used in the work presented here.

With the variable bypass fraction and cleaning, Case III, Figure 6(d) shows that it is possible to maintain the desalter inlet temperature within the desired band over most of the operating period, apart from the last 2 months and the short drops due to cleaning. Whether it is acceptable to have $T_{\rm de}$ drop briefly below the lower control limit during cleaning actions is a question for the refinery operators. In this simulation it is noticeable that the shell-side split fraction of the control HEX is varied 3 times over the 3 year period.

Comparison of the cleaning schedules for Cases II and III shows that there is a rearrangement of cleaning actions before and after the desalter (Figure 6(d)). In the fixed split scenario (Case II) one single HEX is cleaned 3 times. This pattern can be used to identify which HEXs are most sensitive in determining the desalter inlet temperature. Alternatively, the simulator could be used to evaluate which HEX should be selected to be used as the 'control HEX'. The CIT profiles show that Case II focuses more on maintaining a higher CIT.

Table 5 summarizes the performance of the three cases. Apart from the furnace penalty being slightly higher than Case II, the network performance in Case III is considered best in terms of reduced overall fouling penalty, fewer cleaning actions and the capability to maintain $T_{\rm de}$ within the limits for most of the operating period. It should be noted that the results are subject to the relative weighting of the various components in the objective function, *e.g.* cleaning vs. energy costs. Hydraulic performance was modelled in this case study but throughput limitations did not arise.

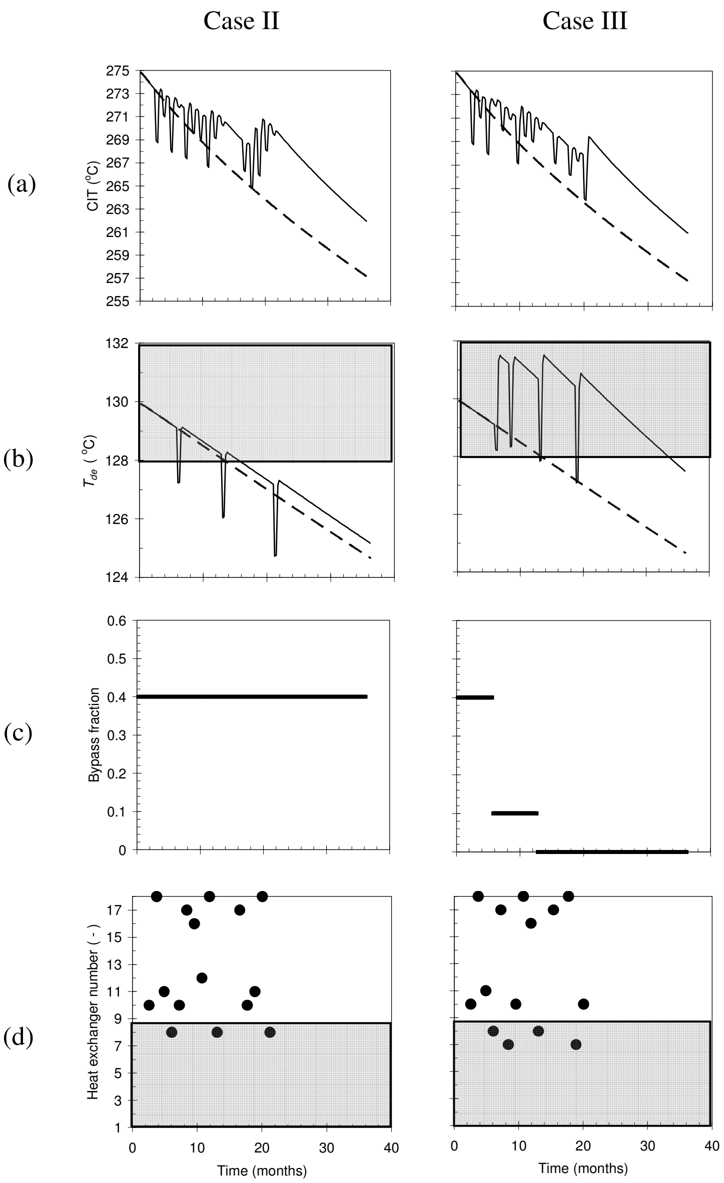


Fig. 6 Simulated network performance: (a) CIT (b) desalter inlet temperature, (c) bypass fraction and (d) cleaning schedule, over a 3 year period. Dashed lines in (a) and (b) represent the base case (Case I, no cleaning or bypass control); in (b) the target operating region of the desalter is highlighted in grey (128 – 132°C); in (d) HEXs upstream of the desalter are highlighted in grey. The HEXs are numbered sequentially in (d) based on Figure 5, such that HEX 18 in (d) corresponds to HEX 9A in Figure 5.

## CONCLUSIONS

We have demonstrated how data readily available for an operating refinery preheat train may be used to plan future operations including cleaning while incorporating important operating constants such as those presented by desalter performance criteria. In particular:

1. A data reconciliation study was performed for an existing crude oil refinery; fouling rates were extracted for different exchangers in the PHT.

2. Analysis of fouling rates revealed that the Ebert-Panchal model could be used to represent fouling in most of the exchangers at the hot end of the PHT.

3. Scheduling of heat exchanger cleaning and a method to control desalter inlet temperature through a heat exchanger bypass manipulation was successfully implemented and applied to a existing refinery case study.

## ACKNOWLEDGEMENTS

Funding from EPSRC project EP/D50306X and financial support for EMI from the Cambridge Overseas Trust is gratefully acknowledged, as well as helpful discussions with Dr. Graham Polley and Simon Pugh of IHS-ESDU.

## NOMENCLATURE

$A$ surface area, $m^2$
$a$ constant (Eq. 2), $m^2K\ J^{-1}$
$b$ constant (Eq. 2), $m^2K\ J^{-1}\ Pa^{-1}$
$C_{c,i}$ cleaning cost for HEX $i$, US\$ unit$^{-1}$
$C_p$ crude specific heat capacity, $J\ kg^{-1}\ K^{-1}$
$C_E$ energy cost, US\$ $MW^{-1}$ day$^{-1}$
$C_{de}$ desalter penalty cost, US\$ day$^{-1}$
$c$ constant (Eq. 11), K
$d$ constant (Eq. 11), K
$d_i$ tube internal diameter, m
$E$ activation energy for fouling, $J\ mol^{-1}$
$f$ parameters in Table 3
$g$ gravitational acceleration, $ms^{-2}$
$G$ greedy decision parameter, US\$
$h$ film heat transfer coefficients, $W\ m^{-2}\ K^{-1}$
$m$ mass flow rate, $kg\ s^{-1}$
$n$ skewness index in Eq. (7), -
$N_c$ number of cleaning actions, -
$N_s$ time horizon, day
$P_{de}$ desalter penalty, -
$Pr$ Prandtl number, -
$Q$ heat duty, MW
$r$ droplet radius, m
$R$ gas constant, $J\ mol^{-1}\ K^{-1}$
$\dot{R}_f$ fouling rate, $m^2K\ J^{-1}$
$R_f$ fouling resistance, $m^2K\ W^{-1}$
$R_w$ tube-wall resistance, $m^2K\ W^{-1}$
$Re$ Reynolds number, -
$T$ temperature, K
$t$ time, s
$t_F$ time horizon for plant shutdown, days
$U$ overall heat transfer coefficient, $W\ m^{-2}\ K^{-1}$
$u_m$ axial mean velocity, $m\ s^{-1}$
$u_s$ settling velocity, $m\ s^{-1}$
$x$ hot stream bypass fraction, -

$\gamma$ estimated benefit from cleaning HEX, US\$
$\Gamma$ total network fouling penalty, US\$
$\delta$ deposit thickness, m
$\Delta_G$ greedy threshold value, US\$
$\Delta t_w$ time window, days
$\varepsilon_i$ effectiveness of HEX $i$
$\lambda_{oil}$ crude thermal conductivity, $W\ m^{-1}\ K^{-1}$

$\mu_{oil}$ viscosity of oil, Pa s
$\upsilon$ kinematic viscosity, $m^2 s^{-1}$
$\rho_{oil}/\rho_w$ density of crude oil/water, kg $m^{-3}$
$\tau_w$ wall shear stress on the inner tube/foulant surface, Pa

**Subscripts**

| | | | |
|---|---|---|---|
| *c* | cold stream ; | *Cl* | clean |
| *cleaning* | cleaning period ; | *De* | desalter |
| *f* | fouled ; | *Film* | tube-side film |
| *h* | hot stream ; | *I* | internal |
| *in* | Inlet ; | *Ne* | network |
| $N_p$ | number of time period; | *O* | outer/external ; |
| *operation* | operating period | *Out* | outlet; |

**Super scripts**

| | | | |
|---|---|---|---|
| * | target; | *H* | upper threshold |
| *L* | lower threshold | | |

**REFERENCES**

B.D. Crittenden, S.T. Kolaczkowski and I.L. Downey, 1992, Fouling of crude oil preheat exchangers. *Chemical Engineering Research and Design,* **70**, 547-557.

ESDU (2000). Heat exchanger fouling in the pre-heat train of a crude oil distillation unit, Data Item 00016, IHS ESDU International plc., London.

A. V. Fiacco and G. P. McCornick, 1968, *Non linear programming: Sequential unconstrained minimization techniques*, Wiley, New York.

M.C. Georgiadis, L.G. Papageorgiou and S. Macchietto, 2000, Optimal cleaning policies in heat exchanger networks under rapid fouling. *Industrial and Engineering Chemistry Research*, **39**, 441-454.

V. Gnielinski, 1976, New equations for heat and mass-transfer in turbulent pipe and channel flow, *International Chemical Engineering*, **16(2)**, 359-368.

G.F. Hewitt, G.L. Shires and T.R. Bott, 1994. *Process Heat Transfer*, 183-184. CRC Press, Inc., Florida, U.S.A.

E.M. Ishiyama, W.R. Paterson and D.I. Wilson, 2008, Thermo-hydraulic channelling in parallel heat exchangers subject to fouling, *Chemical Engineering Science*, **63**(13), 3400-3410.

E.M. Ishiyama, W.R. Paterson and D.I. Wilson, 2009, Platform for techno-economic analysis of fouling mitigation options in refinery preheat trains, *Energy & Fuels,* **23**(3), 1323-1337.

J.H. Lavaja and M.J. Bagajewicz, 2004, On a new MILP model for the planning of heat exchanger network cleaning. *Industrial and Engineering Chemistry Research,* **43**, 3924-3938.

Y. Li and A.P. Watkinson, 2008, Characteristic of Heavy vacuum gas oil fouling in the presence of dissolved oxygen, in proceedings of *9th International Conference on Petroleum Phase Behaviour and Fouling,* Victoria, Canada.

G.T. Polley, D.I. Wilson, B.L. Yeap and S.J. Pugh, 2002, Evaluation of laboratory crude oil threshold fouling for application to refinery preheat trains. *Applied Thermal Engineering.,* **22**, 777-788.

G.T. Polley, A. Morales-Fuentes and D.I. Wilson, 2009, Simultaneous consideration of flow and thermal effects of fouling in crude oil preheat trains, *Heat Transfer Engineering*, **30**(10-11), 815-821.

E.F. Pruneda, E.R.B. Escobedo and F.J.G. Vazquez, 2005. Optimum temperature in the electrostatic desalting of Maya crude oil, *Journal of Mexican Chemical Society*, **49(1)**, 14-19.

C. Rodriguez and R. Smith, 2007, Optimization of operating conditions for mitigating fouling in heat exchanger networks, *Chemical Engineering Research and Design,* **85**, 839-851.

F. Smaïli, V.S. Vassiliadis and D.I. Wilson, D.I., 2001, Mitigation of fouling in refinery heat exchanger networks by optimal management of cleaning. *Energy & Fuel,* **15**, 1038-1056.

J. Sousa, M. da Conceição and A. Sá Marques, 1999. An explicit solution to the Colebrook-White equation through simulated annealing, in *Water Industry Systems: Modelling and Optimization Applications (volume two)*, 347-355. Research Studies Press Ltd., Baldock, Hertfordshire.

D.I. Wilson, F. Smaïli and V.S. Vassiliadis, 2000, Mitigating of fouling in refinery pre-heat trains by optimal management of cleaning and antifoulant treatment, in proceedings of *Second International Conference on Petroleum Phase Behaviour and Fouling,* Copenhagen, Denmark.

B.L. Yeap, D.I. Wilson, G.T. Polley and S.J. Pugh, 2004, Mitigation of crude oil refinery heat exchanger fouling through retrofits based on thermo-hydraulic fouling models, *Chemical Engineering Research and Design,* **82(A1)**, 53-71.

Table 2: Thermo-physical properties of crude oil.

| Parameter | Value |
|---|---|
| Density, kg $m^{-3}$ | $\rho = 931.65 - 0.6597T$ |
| Specific heat capacity, J $kg^{-1}$ $K^{-1}$ | $C_p = 1959.66 + 3.1093T$ |
| Thermal conductivity, W $m^{-1}$ $K^{-1}$ | $\lambda_{oil} = 0.1749 - 0.0002T$ |
| Dynamic viscosity, mPa s | $\mu_{oil} = 1498.7\,T^{-1.5611}$ |

Temperature, $T$ in °C.

Table 3: Fouling resistance and fouling rate correlations

| | Fouling resistance | Fouling rate |
|---|---|---|
| Linear | $f_1 + f_2 t$ | $f_2$ |
| Kern & Seaton | $f_3[1-\exp(-f_4 t)]$ | $f_3 f_4 \exp(-f_4 t)$ |
| Falling rate | $f_5 \ln(t) - f_6$ | $f_5/t$ |

Here $f_i$ are dimensional constants and $t$ is the time.

Table 4: Summary of fouling rates in each heat exchanger

| HEX | Fouling behaviour | Fouling rate ($m^2K/J$) |
|---|---|---|
| 1-5 | Linear | $f_2 = 5.00\times10^{-12}$ |
| 6AB | Linear | $f_2 = 9.95\times10^{-11}$ |
| desalter | ---------- | ---------- |
| 8A | Linear | $f_2 = 2.66\times10^{-11}$ |
| 8B | Linear | $f_2 = 6.19\times10^{-11}$ |
| 8C | Linear | $f_2 = 7.21\times10^{-11}$ |
| 8D | Linear | $f_2 = 1.32\times10^{-10}$ |
| 7, 9A-E | Chemical reaction | $a = 926\ m^2K\ kW^{-1}\ h^{-1}$<br>$\gamma = 4.3\times10^{-8}\ m^2K\ kW^{-1}\ h^{-1}\ Pa^{-1}$<br>$E = 36.4\ kJ\ mol^{-1}$ |

Table 5: Summary of case study PHT performance under different operational strategies

| | Case I | Case II | Case III |
|---|---|---|---|
| Desalter penalty, k$US | 327 | 272 | 50 |
| Furnace penalty, k$US | 1,763 | 1,161 | 1,232 |
| Cleaning actions | 0 | 15 | 14 |
| Total cleaning cost, k$US | 0 | 150 | 140 |
| $T_{de}$ control span, months | 12 | 13 | 34 |
| Total penalty, M$US | 2.1 | 1.6 | 1.4 |

Table 1: Summary of heat exchanger details: clean operation. (Average crude oil flow rate of 109.8 kg $s^{-1}$)

| | Heat exchanger number 1,2 | 3A,B | 4 | 5 | 6A,B | 7 | 8A-D | 9A-E |
|---|---|---|---|---|---|---|---|---|
| $A_o$ ($m^2$) [each unit] | 237.2 | 372.4 | 237 | 390.6 | 456.3 | 660.8 | 309.6 | 376.8 |
| Tube passes | 2 | 2 | 2 | 2 | 2 | 2 | 2 | 2 |
| Number of tubes | 810 | 1020 | 900 | 1070 | 1250 | 1810 | 848 | 1032 |
| Average crude velocity (m $s^{-1}$) | 1.76 | 1.43 | 1.64 | 1.39 | 1.19 | 0.83 | 1.84 | 1.32 |
| Average *Re* | 8,700 | 13,700 | 20,300 | 19,000 | 18,000 | 15,000 | 49,000 | 47,000 |
| *Pr* | 40 | 19 | 15 | 14 | 13 | 11 | 8 | 7 |
| Product flow rate (kg $s^{-1}$) | 18.5 | 48.7 | 95.9 | 5.8 | 18.5 | 57.1 | 117.4 | 47.7 |
| Hot stream $C_p$ (kJ $kg^{-1}$ $K^{-1}$) | 2500 | 2640 | 2500 | 2400 | 2500 | 2680 | 2810 | 2560 |
| $U$ (W $m^{-2}$ $K^{-1}$) | 479 | 142 | 442 | 108 | 109 | 126 | 178 | 545 |